

# Experimental investigation of the dynamics of kinks of dislocation lines in semiconductor single crystals

V.I. Nikitenko, B. Ya. Farber, and Yu. L. Iunin

*Institute of Solid-State Physics, Academy of Sciences of the USSR, Chernogolovka, Moscow Province*

(Submitted 15 January 1987)

Zh. Eksp. Teor. Fiz. **93**, 1304–1318 (October 1987)

Information on the dynamic properties of kinks (topological solitons), governing the mobility of dislocations in a Peierls relief, was obtained by investigating the laws governing the motion of individual  $60^\circ$  and screw dislocations in silicon single crystals subjected to a periodic pulsed loading. Studies were made of the dependence of the average glide distance of dislocations on the pulse length and repetition rate. The proposed model for the analysis of the experimental data made it possible to estimate the principal characteristics of the processes of formation, diffusion, and drift of kinks. The temperature dependences of the dislocation velocities and of the kink diffusion coefficient were determined and the effective activation energies of the formation and migration of kinks were found independently. A strong influence of the steepness of the leading edge of the load pulses on the average dislocation glide distance was observed. The results obtained were compared with the existing theories of dislocation motion in a deep potential relief of the crystal lattice. Serious discrepancies were found between the experimental data and theoretical predictions. The reasons for the discrepancies were analyzed and an attempt was made to account for them by considering the influence of impurities and dynamic solitons on the formation of kink pairs and on their expansion along a dislocation line.

## INTRODUCTION

The translational symmetry of the crystal lattice is responsible for the existence of potential barriers  $W_p(z)$  hindering dislocation motion (Fig. 1). The application of stresses lower than the Peierls stress  $\sigma_p = (\partial W_p / \partial z)_{\max} / b$ , where  $b$  is the Burgers vector, induces transfer of dislocations between neighboring valleys of the potential relief by formation of kink and antikink pairs as a result of thermal fluctuations and subsequent expansion of a pair to the ends of a dislocation segment or until annihilation takes place with kinks of the opposite sign in neighboring pairs (Fig. 1a). A theory of this process is quite well advanced.<sup>1-7</sup> It has been checked experimentally by investigating the mobilities of single dislocations in single crystals of elementary semiconductors,<sup>8-16</sup> characterized by extremely high Peierls barriers, and a number of discrepancies have been found between the experimental results and theoretical predictions.<sup>10,14-18</sup> The resolution of these conflicts will require separate experimental studies of the processes of formation of kink pairs and of their expansion along a dislocation line.

We proposed earlier<sup>19,20</sup> a method which can ensure a time resolution sufficient for the investigation of the various stages of the process of transfer of a dislocation between neighboring valleys of the potential relief which opens up prospects for solving the problem stated above. The method

is based on an investigation of the mobility of single dislocations under the action of a succession of load pulses. The duration of each pulse  $t_i$  is comparable with the average time for the transfer of a dislocation to an adjacent valley of the potential relief,  $t_a = a/v_d$ , where  $a$  is the distance between the valleys of the relief and  $v_d$  is the velocity of steady-state motion of dislocations measured under a static load. The load pulses are separated by pauses of duration  $t_p$  when no stress is applied ( $\sigma = 0$ ). Formation and expansion of kink pairs on a dislocation line occurs during a load pulse. If during such a pulse the kinks of opposite signs in neighboring pairs do not annihilate, then during the next pause (after removal of the load) the resultant double kinks become unstable and contract toward their nucleation centers. If the pause is sufficiently long, the double kinks contract completely. When these double kinks make a decisive contribution to the velocity of a dislocation, the glide distance is practically equal to zero irrespective of the number of loading cycles. However, if the duration of the pause is insufficient to complete the relaxation process, kink pairs expand under the action of the subsequent load pulses, so that in the final analysis a dislocation is displaced by a macroscopic distance because of the repeated application of the load pulses.

It therefore follows that varying the duration of the load pulses and of pauses between them and using displacement

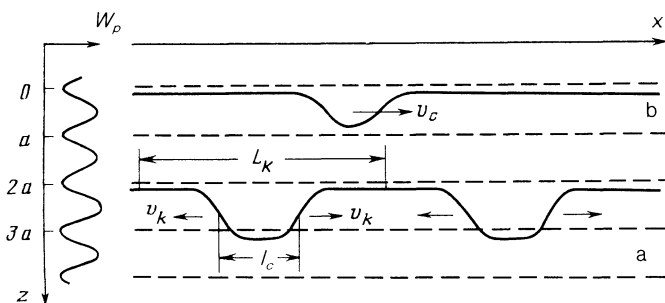


FIG. 1. a) Overcoming a Peierls barrier  $W_p(z)$  by a dislocation at stresses below the Peierls stress. b) Nonlinear excitation in the form of a solitary wave (dynamic soliton).

of dislocations as an indicator can provide information on the characteristic times of the formation of a pair of kinks and its expansion until annihilation, and also on the characteristics of the motion of a kink along a dislocation line. Then, subject to very general assumptions about the nature of motion of kinks along a dislocation line, it is possible to estimate all the principal characteristics of the processes of nucleation and migration of kinks along a dislocation.

We have used this method of periodic pulsed loading to investigate the mobility of single dislocations of different types in silicon single crystals. The experimental results were used to estimate the diffusion coefficient, drift velocity of kinks along a dislocation line, and the concentration of kinks. We measured the temperature dependence of the velocity of  $60^\circ$  dislocations and of the kink diffusion coefficient, and found independently the effective activation energies of the formation and migration of kinks. The steepness of the leading edge of the load pulses had a significant influence on the process of formation of kink pairs, which provided an opportunity of identifying the mechanisms by which nonlinear excitations form on dislocations, governing the motion of the latter in semiconductor single crystals.

### EXPERIMENTAL METHOD

We investigated rectangular rods with the  $[1\bar{1}0]$ ,  $[11\bar{2}]$ , and  $[111]$  orientations and  $35 \times 4 \times 1.5$  mm dimensions, which were cut from dislocation-free ingots of *n*-type silicon grown by the floating zone method and doped during growth with phosphorus until a resistivity of  $\sim 150 \Omega \cdot \text{cm}$  was reached. When single dislocations were introduced into a sample, a diamond indenter was used to form scratches on the opposite  $\{111\}$  surfaces parallel to the  $[1\bar{1}0]$  edge. The sample was then subjected to four-point bending. The bending axis coincided with the  $[11\bar{2}]$  direction. During the first loading at  $T = 600^\circ \text{C}$  by a stress of  $\sigma = 3 \text{ kg/mm}^2$  it was found that dislocation half-loops of semihexagonal shape were created near the scratches on the compressed and stretched sides of the sample. Segments of these half-loops emerging on the surface of the sample on different sides of a scratch had either just the  $60^\circ$  orientation (Fig. 2a) or the  $60^\circ$  and screw orientations (Fig. 2b). Under these deformation conditions we could readily determine<sup>21</sup> the position of dislocations known to have the  $60^\circ$  orientation (types 2 and 4 in Fig. 2) relative to a scratch. Moreover, the use of Sirtl's etchant for revealing dislocations made it possible to distinguish unequivocally the  $60^\circ$  and screw dislocations on the basis of the shape of the etch pits.<sup>22</sup>

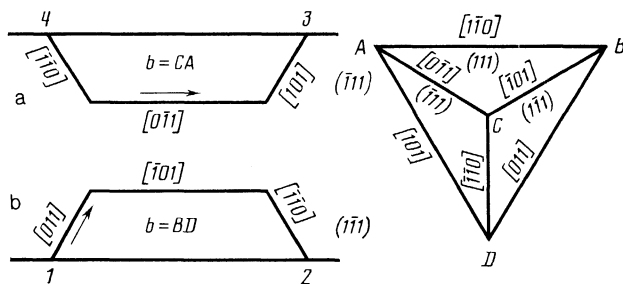


FIG. 2. Types of dislocation half-loops used in experiments: a) half-loops in the slip system  $(\bar{1}\bar{1}1) [011]$  introduced on the stretched side; b) half-loops in the slip system  $(\bar{1}\bar{1}1) [011]$  introduced on the compressed side. The orientation of the Thompson tetrahedron is shown on the right.

During the subsequent loading the newly formed dislocation half-loops expanded to a diameter of  $800\text{--}1000 \mu\text{m}$ . The crystal was then cooled and etched again; it was then used as the starting sample in the subsequent experiments. It should be pointed out that we determined the glide distances only of those  $60^\circ$  or screw segments of dislocation half-loops which showed no surface bending.<sup>21</sup>

A sample was deformed by four-point bending. Mechanical load pulses were applied as follows. A trapezoidal signal from a generator of pulses of special shape was applied to a transistor switch, which controlled the current in an electromagnetic force transducer. The transducer was in the form of two planar coils connected facing one another with a permanent magnet (made of  $\text{SmCo}_5$  alloy) placed between them. The force transmitted to the sample by the magnet was measured with a piezoelectric ceramic sensor located in the cold zone of the apparatus. This sensor was calibrated before each loading. Separate experiments established that the profile and amplitude of the signal obtained from the piezoelectric ceramic sensor agreed with the profile and amplitude of the signal recorded using strain gauges bonded to a calibration beam. Special measures were taken to avoid a constant component of the load in the pauses between the pulses, when the applied stress should be zero. This was done by employing a magnetic suspension of the components of the loading device.

This method made it possible to create a sequence of load pulses with the duration of a single pulse ranging from 5 msec to 1 sec and pulse rise times from 0.5 to 10 ms. In the large-scale experiments the rise time of the load pulses,  $t_f$ , was 4 ms. Moreover, we investigated the influence of the slope of the leading edge of the load pulses on the laws governing the motion of dislocations in a sample subjected to periodic pulsed loading. The duration of active loading, i.e., the total duration of the load pulses, was selected to be equal to the static loading during which dislocations traveled a distance  $\bar{l}_{st} \approx 20\text{--}30 \mu\text{m}$ . The temperature during deformation was measured by a thermocouple placed in the immediate vicinity of a sample and this temperature was kept constant to within  $\pm 1 \text{ K}$ .

### EXPERIMENTAL RESULTS

In earlier papers<sup>19,20</sup> we reported the results of an investigation of the mobility of  $60^\circ$  dislocations under conditions of periodic pulsed loading with tensile stresses. In the present case we studied not only  $60^\circ$  but also screw segments of dislocation half-loops located in the compressed and stretched parts of a sample.

Figure 3 shows the dependences of the average glide distance  $\bar{l}$  of dislocations of all four types (normalized to the average glide distance measured in the static experiment) on the relative duration of the load pulses (in units of the time  $t_a$  needed to transfer to the next valley each separate type of dislocation) when the inverse-duty factor was  $Q = 2$  (i.e.,  $t_p = t_i$ ). The temperature during our tests was  $T = 600^\circ \text{C}$ , the reduced tangential stress was  $\sigma = 0.7 \text{ kg/mm}^2$ , the duration of active loading was  $\sum t_i = t_{st} = 7200 \text{ s}$ , and the rise time of the pulses was  $t_f = 4 \text{ ms}$ . Clearly, the dependences were similar for all types of dislocations and, in first order, they could be described by a single curve. In the range of short pulse lengths ( $t_i/t_a < 0.2$ ) we found that  $\bar{l} = 0$ , where-

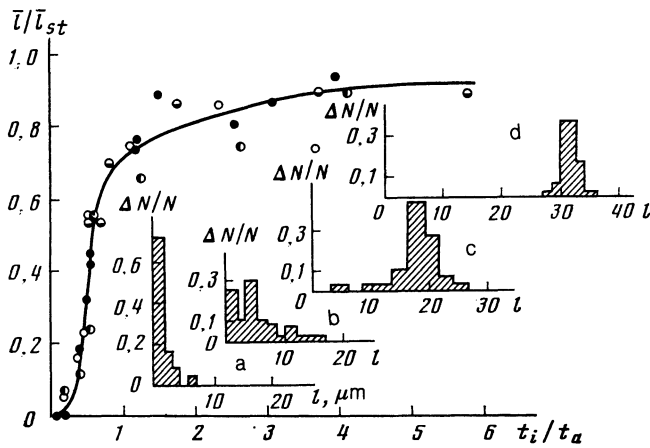


FIG. 3. Dependences of the normalized average glide distance of dislocations ( $\bar{l}/\bar{l}_{st}$ ) on the relative duration of the load pulses ( $t_i/t_a$ ) obtained on condition that  $t_p = t_i$  for dislocations of four types shown in Fig. 2: (●) type 1; (●) type 2; (○) type 3; (○) type 4. The insets show oscillograms of the glide distances traveled by  $60^\circ$  dislocations (type 3 in Fig. 2) under load pulses of different durations: a)  $t_i/t_a = 0.2$ ; b)  $t_i/t_a = 0.5$ ; c)  $t_i/t_a = 0.6$ ; d) static loading. Conditions during loading:  $T = 600^\circ\text{C}$ ,  $\sigma = 0.7 \text{ kg/mm}^2$ ,  $\Sigma t_i = t_{st} = 7200 \text{ s}$ ,  $t_f = 4 \text{ ms}$ .

as in the range  $0.2 < t_i/t_a < 0.7$  the average glide distance rose rapidly from a point of inflection at  $t_i/t_a \approx 0.5$ , but in the range  $t_i/t_a > 0.7$  this was followed by an extended region of slow approach to the values obtained under static loading, which was reached at  $t_i/t_a \approx 6-8$ .

In the region where  $\bar{l}(t_i)$  varied rapidly, all types of dislocations exhibited radical changes in the nature of the distribution of the dislocation glide distances. The insets in Fig. 3 are typical histograms of the glide distances of  $60^\circ$  dislocations (type 3 in Fig. 2). The histogram *a* represents the onset of the rapid rise of the dislocation glide distance with increasing duration of the load pulses ( $t_i/t_a = 0.2$ ), the histogram *b* corresponds to the point of inflection of the  $\bar{l}(t_i)$  curve ( $t_i/t_a = 0.5$ ), and the histogram *c* is obtained in the region of the transition from the strong to the weak dependence  $\bar{l}(t_i)$  ( $t_i/t_a = 0.6$ ). The histogram *d* describes the distribution of the dislocation glide distances in a sample subjected to a static load.

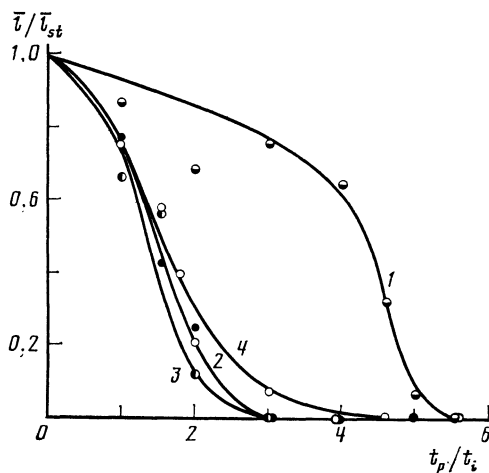


FIG. 4. Dependences of the normalized average glide distance of dislocations on the duration of the pauses (in units of  $t_p/t_i$ ) obtained for dislocations of four types shown in Fig. 2 (the curves are numbered in the same way as the types of dislocations);  $t_i = \text{const} = 94 \text{ ms}$ ,  $T = 600^\circ\text{C}$ ,  $\sigma = 0.7 \text{ kg/mm}^2$ ,  $\Sigma t_i = t_{st} = 7200 \text{ s}$ ,  $t_f = 4 \text{ ms}$ .

Figure 4 shows how the normalized average glide distance of the four types of dislocations depend on the relative duration of the pauses ( $t_p/t_i$ ) when the pulse length was fixed at  $t_i = 94 \text{ ms}$ , corresponding to different values of  $t_i/t_a$  for dislocations of different types because of the differences in the steady-state velocities. The values of the ratio  $t_i/t_a$  were 1.8, 1.24, 1.29, and 1.15 for curves 1, 2, 3, and 4, respectively. Clearly, all four dependences were qualitatively similar. An increase in the duration of the pause reduced monotonically the dislocation glide distance from  $\bar{l}_{st}$  to zero and the values of the critical pause length  $t_p^*$  at which the reduction in the dislocation glide distance was strongest (corresponding to the points of inflection of curves 1-4) were approximately the same for all types of  $60^\circ$  dislocations (curves 2-4), but differed considerably from  $t_p^*$  obtained for screw dislocations (curve 1).

When the duration of the pauses was increased (with  $t_i$  held constant) we again observed significant changes in the nature of the histograms representing the average dislocation glide distances (similar to those in the insets in Fig. 3). In the dependence  $\bar{l}(t_p)$  was weak the dislocation glide distances decreased monotonically. In the region of the strong dependence  $\bar{l}(t_p)$  the histograms changed qualitatively and unshifted dislocations appeared so that near the point of inflection of the curves 1-4 the histograms exhibited two peaks. A further increase in  $t_p$  increased the number of unshifted dislocations and when the pause was long enough all dislocations stopped completely.

## DISCUSSION OF RESULTS

The theory of motion of dislocations in a Peierls relief has been developed to the greatest extent for relatively small applied stresses  $\sigma \lesssim 0.1 \sigma_p$ ,<sup>1-3,5,7</sup> and analytic expressions have been obtained for the velocity of steady-state motion of dislocations, which can be compared directly with the experimental data obtained under static loading conditions. The theory is based on the assumption that a dislocation moves as a result of formation and expansion of pairs of kinks and that the mobility of kinks along a dislocation line is governed by the diffusion and drift processes. It is assumed that at temperatures other than absolute zero an equilibrium concentration of kinks  $c_k$  is established on a dislocation because of thermal fluctuations and this is true even in the absence of a stress:

$$c_k = (2/b) \exp(-U_k/kT), \quad (1)$$

where  $U_k$  is the energy of a single kink,  $k$  is the Boltzmann constant, and  $T$  is the absolute temperature. Application of an external stress results in directional drift of kinks at a velocity

$$v_k = (D_k/kT) \sigma a b, \quad (2)$$

where

$$D_k = \nu_D b^2 \exp[-W_m(\sigma)/kT] \quad (3)$$

is the kink diffusion coefficient,  $W_m(\sigma)$  is the activation energy for migration of a kink along a dislocation line (curve 3 in Fig. 5), and  $\nu_D$  is the Debye frequency.

In the range of very low stresses the concentration of kinks is practically independent of the stress  $\sigma$  and the mini-

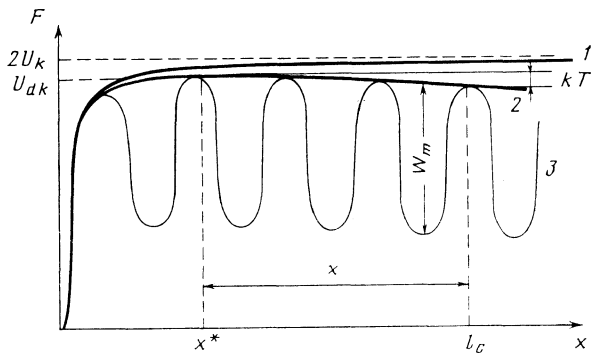


FIG. 5. Dependences of the free energy of a pair of kinks on the distance between them in the absence of a load ( $\sigma = 0$ , curve 1) and in the presence of a load ( $\sigma \neq 0$ , curve 2), and in the presence of high barriers  $W_m \gg kT$  hindering kink motion (curved 3).

imum velocity of a dislocation is limited by the concentration of kinks in thermal equilibrium:

$$v_d^m = a c_k v_k. \quad (4)$$

When the applied stress is increased, the concentration of kinks on a dislocation line increases because of the formation of additional kink pairs. The motion of dislocations is influenced only by stable pairs which have reached the size

$$l_c = x^* + x', \quad (5)$$

where

$$x^* = (\alpha / \sigma ab)^{1/2} \quad (6)$$

and

$$x' = kT / \sigma ab, \quad (7)$$

and  $\alpha$  is the constant of the elastic interaction between kinks forming a pair.

At a critical distance  $x^*$  the mutual attraction between kinks is balanced out by the external force. At this point the energy of a double kink

$$F(x) = 2U_k - \alpha/x - \sigma abx \quad (8)$$

has its maximum value (Fig. 5)

$$U_{dk} = 2U_k - 2(\alpha ab \sigma)^{1/2}, \quad (9)$$

where  $x'$  is the distance from a saddle point (denoted  $x^*$ ) over which the energy  $U_{dk}$  decreases by  $kT$  (curve 2 in Fig. 5). Collapse of a double kink of size  $x > l_c$  requires a fluctuation of energy greater than  $kT$  and the probability of this process is low. In the case of kink pairs of size  $x > l_c$  expansion is favored energetically under the action of external forces until the ends of a dislocation segment are reached or until annihilation takes place between kinks of opposite sign in neighboring pairs. The process by which a double kink grows from  $x^*$  to  $l_c$  is governed by a random walk of the kink along a dislocation, since the work done by external forces in the course of expansion of a double kink to a distance  $x < x'$  is less than  $kT$ .

A static load establishes a steady-state kink flux  $J$  across a barrier  $U_{dk}(\sigma)$  and this flux determines the probability of formation of a stable double kink per unit time and per unit length of a dislocation line:

$$J = \frac{D_k \sigma a}{2bkT} \exp[-U_{dk}(\sigma)/kT]. \quad (10)$$

The velocity of steady-state motion of a dislocation is then given by

$$v_d = aJL. \quad (11)$$

Using the steady-state condition

$$L_K / 2v_k = 1/JL_K, \quad (12)$$

we can determine the mean free path  $L_K = (2v_k/J)^{1/2}$  of a kink until annihilation and the velocity of steady-state motion of long ( $L > L_K$ ) dislocations:

$$v_d = a(2v_k J)^{1/2} = \frac{b^2 v_D \sigma a^2}{kT} \exp\left[-\frac{U_{dk}(\sigma)/2 + W(\sigma)}{kT}\right]. \quad (13)$$

These formulas can be compared directly with the results of a determination of the dislocation velocity under static load conditions. In the case of periodic pulse loading for  $t_i \leq t_a$  the steady-state condition is not satisfied, so that kink pairs created during a load pulse do not expand sufficiently for annihilation with neighboring kinks during a single pulse. Therefore, the results obtained cannot be analyzed using the final expressions for  $J$  and  $v_d$  given by Eqs. (10) and (13), so that it is necessary to develop a model for the analysis of the experimental data in order to obtain quantitative information on the mechanisms limiting the mobility of dislocations in the Peierls relief. We shall construct this model using the most general assumptions of the earlier theories that the motion of a kink along a dislocation line is governed by diffusion and drift processes, and the main contribution to the motion of dislocations comes only from stable pairs of kinks of size  $x > l_c$ .

Figure 6 shows schematically the distance between kinks in a pair as a function of the loading time, and also of the pause between the pulses. In the case of periodic pulsed loading the time  $t_i$  for a dislocation to pass to an adjacent value of the potential relief includes the time  $\tau_f$  of formation of a stable double kink and the time  $\tau_m$  for this double kink to expand to the ends of a dislocation segment or until it annihilates with neighboring kinks:  $t_i = \tau_f + \tau_m$ .

It follows from the theories of Refs. 1 and 2 that the formation of a stable double kink of size  $l_c$  is governed by its diffusive expansion from  $x^*$  to  $l_c$  because of a random walk along a dislocation line of the kinks forming a pair. The mu-

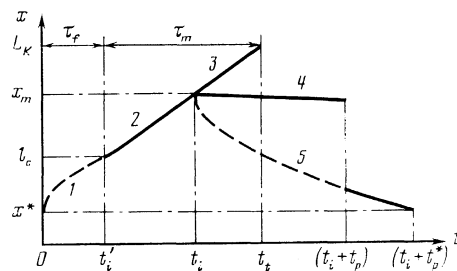


FIG. 6. Relative displacements of kinks in a pair plotted as a function of time during application of a load ( $t_i$ ) and in the pause between load pulses ( $t_i + t_p$ ): 1) diffusion spreading of a pair to its critical size; 2) drift broadening of a pair of kinks in the field of external forces; 3) drift broadening of a pair until annihilation with kinks in neighboring pairs; 4) estimate of the drift contraction of a pair of kinks in the field of forces of mutual attraction ( $\alpha/x^3$ ); 5) contraction of a pair of kinks due to diffusion.

tual displacement of kinks during a load pulse (curve 1 in Fig. 6) can be calculated from

$$\Delta x = (2D_p t_i)^{1/2}, \quad (14)$$

where  $D_p = 2D_k$  is the diffusion coefficient of a pair of kinks.

In the diffusion regime expansion and contraction of a double kink are both equally probable. Therefore, when experiments are carried out keeping the pulse length and the pause equal, it is possible to identify when the transition from diffusion to drift of kinks in a field of external forces occurs, because such a change in the kink motion mechanism means that double kinks do not contract to the nucleation center during a pause and a dislocation travels a macroscopic distance as a result of repeated pulsed loading. Then, if  $t_i < \tau_f$ , the average glide distance of dislocations  $\bar{l}$  should vanish. When  $t_i$  is increased, it rises in steps and reaches its static value for  $t_i > \tau_f$ . However, the process by which a double kink forms is random. Therefore, the critical value of  $t_i$  is associated not with an abrupt transition from 0 to  $\bar{l}_{st}$ , but with the point of inflection of the curve in Fig. 3. It follows that in the time  $t_i^*$  the distance between the kinks in a pair increase by  $x'$ . We can then obtain the following estimate from Eq. (14):

$$D_p = (x')^2 / 2t_i'. \quad (15)$$

Under specific experimental conditions we have  $T = 600^\circ\text{C}$  and  $\sigma = 0.7 \text{ kg/mm}^2$ ; Eqs. (6) and (7) yield  $x^* = 19b$  and  $x' = 35b$ . The curve in Fig. 3 gives  $t_i' \approx 38 \text{ ms}$  for  $60^\circ$  dislocations of type 2 (Fig. 2) and then Eq. (15) yields  $D_p = 2.4 \times 10^{-11} \text{ cm}^2 \text{ s}^{-1}$  and  $D_k = 1.2 \times 10^{-11} \text{ cm}^2 \text{ s}^{-1}$ .

The drift velocity of a kink can be estimated from the experimental dependence  $\bar{l}(t_p)$ . If the pulse length is sufficiently long that  $\tau_f < t_i < t_r$ , double kinks can diffuse to the critical size and then they expand by drift under the action of an external force (curve 2 in Fig. 6). When the load is removed, double kinks become unstable and they begin to contract to their nucleation center. If the pause is sufficiently long ( $t_p > t_i$ ), then the double kinks that have not become annihilated with the kinks in the neighboring pairs can contract during a pause completely to the nucleation center and at the beginning of the next loading cycle no stable double kinks remain on a dislocation line, in which case the glide distance of a dislocation during the whole loading time is practically zero. This corresponds to the right most parts of the curves in Fig. 4. If under these conditions the pause is insufficiently long, the process of relaxation is incomplete and double kinks capable of expanding under the action of subsequent load pulses remain on the dislocation line, which ensures macroscopic displacements of dislocations under the influence of repeated pulsed loading. If we ignore the statistics of the distribution of the kink sizes, the critical condition, when the distance traveled by a kink from its nucleation center during a pulse is equal to the distance traveled in the course of contraction during a pause, would imply an abrupt change in  $\bar{l}$  from  $\bar{l}_{st}$  to 0. In Fig. 4 this condition corresponds to the inflection point  $t_p^*$ .

It is clear from Fig. 6 that  $x_m - x^* = x' + 2v_k(t_i - \tau_f)$ . Contraction of double kinks during the pause time is governed either by drift in the field of kink attraction forces ( $\alpha/x^2$ ) (curve 4 in Fig. 6) or by diffusion

(curve 5). Estimates indicate that if we use  $D_p$  deduced from Eq. (15), then the diffusion mechanism for contraction of a double kink predominates and we have  $\Delta x \sim (2D_p t_p)^{1/2}$ . Equating then  $\tau_f = t_i'$  and  $t_p = t_p^*$ , we obtain an equation

$$x' + 2v_k(t_i - t_i') = (2D_p t_p^*)^{1/2}, \quad (16)$$

from which we can calculate  $v_k$ . Having found  $t_p^* = 169 \text{ ms}$  from curve 2 in Fig. 4 and substituted  $D_p$  from Eq. (15), we obtain  $v_k = 1.33 \times 10^{-5} \text{ cm s}^{-1}$ . Knowing  $v_k$  we can obtain once again the estimate  $D_k = 1.8 \times 10^{-11} \text{ cm}^2 \text{ s}^{-1}$  from Eq. (2), which is in satisfactory agreement with the estimate obtained from Eq. (15). This shows that the processes by which a double kink grows to the critical size and its subsequent drift expansion are governed by the same type of barrier. Using the value of  $D_k$  deduced from Eq. (15), we can calculate from Eq. (3) the energy of migration of a kink along a dislocation line:

$$W_m = kT \ln(\nu_D b^2 / D_k) \approx 1.6 \text{ eV}. \quad (17)$$

The migration energy of a kink along a dislocation line was determined directly also from the temperature dependence of the diffusion coefficient of kinks. The position of the point of inflection and the region of strong  $\bar{l}(t_i)$  dependence were determined at temperatures in the range  $550\text{--}625^\circ\text{C}$  using typical histograms of the dislocation glide distances obtained at the boundaries of this temperature range and at the point of inflection (Fig. 3). Equation (15) was used to estimate the diffusion coefficient at each of these temperatures. The point of inflection then corresponded to the average value of  $D_p$  and the boundaries of the region where  $\bar{l}(t_i)$  varies rapidly corresponded to the confidence limit for  $D_p$ .

Figure 7 shows the temperature dependence of the diffusion coefficient of kinks (curve 1) and of the velocities of  $60^\circ$  dislocations of type 2 (curve 2 in Fig. 2). Clearly, the dependences  $\log D_p(1/T)$  and  $\log v_d(1/T)$  can be approximated by straight lines. An analysis by the method of least squares gave the effective migration energy of a kink  $W_m = 1.8 \pm 0.22 \text{ eV}$  and the effective energy of migration of a dislocation  $U_{\text{eff}} = 2.13 \pm 0.11 \text{ eV}$ .

Therefore, within the confidence limit, the activation energy of the motion of a kink calculated from the slope of the temperature dependence agreed with the estimate obtained from Eq. (17). Consequently the preexponential fac-

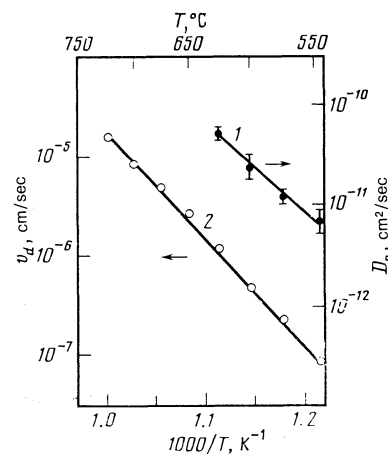


FIG. 7. Temperature dependences of the diffusion coefficient of a pair of kinks (1) and of the dislocation velocity (2);  $\sigma = 0.7 \text{ kg/mm}^2$ ,  $t_f = 4 \text{ ms}$ .

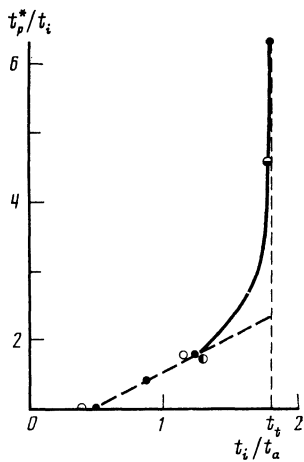


FIG. 8. Dependence of the relative critical duration of a pause ( $t_p^*/t_i$ ) on the pulse length (in units of  $t_i/t_a$ ) for types of dislocations shown in Fig. 2: (●) type 1; (■) type 2; (○) type 3; (□) type 4. The dashed line represents the calculated dependence obtained from Eq. (16);  $T = 600^\circ\text{C}$ ,  $\sigma = 0.7$  kg/mm<sup>2</sup>,  $t_f = 4$  ms,  $\Sigma t_i = t_{st} = 7200$  s.

tor in Eq. (3) had the correct order of magnitude. It should be pointed out that the precision of the determination of  $W_m$  from the slope of the temperature dependence was relatively low, which was due to the fairly large scatter of the experimental data and to the narrow temperature range. Therefore, in further calculations we used the value  $W_m = 1.6$  eV estimated from Eq. (17).

In our model of the motion of dislocations under the influence of periodic pulsed loading we ignored the interaction between kinks in neighboring pairs on a dislocation line. However, in the case of pulses of duration  $t_i > t_a$ , when a double kink can expand to a relatively large size, the annihilation of kinks in neighboring pairs during a pause is more likely than the contraction of a double kink to its nucleation center. Consequently, a dislocation may pass completely to a neighboring valley and will not return to its initial valley no matter how long the pause. This process is indeed observed in experiments. Figure 8 gives the dependence of the critical pause duration  $t_p^*$  (in units of  $t_i$ ) on the relative duration of a pulse ( $t_i/t_a$ ). This dependence was plotted by determining the positions of the points of inflection of the  $\bar{l}(t_p)$  curves similar to those shown in Fig. 4, obtained for different relative durations of the pulses. Clearly, in the case of low values of  $t_i/t_a$  ( $< 1$ ) the experimental results agree quite well with the theoretical (dashed curve) dependence  $t_p^*(t_i)$  obtained from Eq. (16). However, in the range of large values of the ratio  $t_i/t_a > 1.4$  the experimental points deviate considerably from the calculated curve. The vertical asymptote to the experimental curve ( $t_i \approx 1.8t_a$ ) should then correspond to the time taken by a kink to travel until it becomes annihilated with a kink in a neighboring pair, i.e., to the time required for a dislocation to pass completely a neighboring valley of the potential relief. We can then see from Fig. 8 that the time  $t_i$  determined in experiments using pulsed loading is quite close to the average time  $t_a$  for the displacement of a dislocation by one lattice parameter under static loading conditions.

Using the values of  $t_i$  and  $v_k$  obtained in this way, we can employ Eq. (16) to obtain an estimate of the distance

traveled by kinks until annihilation under pulsed loading conditions:

$$L_k = l_c + 2v_k(t_i - t_i') = 122b = 4.6 \cdot 10^{-2} \mu\text{m}. \quad (18)$$

This in turn makes it possible to estimate the steady-state velocity of a dislocation under static loading. Using the steady-state condition of Eq. (12), we find  $J = 2v_k/L_k^2$  and  $v_d = 1.9 \times 10^{-7}$  cm s<sup>-1</sup>. The experimentally determined velocity of a dislocation under a static load is  $\sim 4 \times 10^{-7}$  cm s<sup>-1</sup>, which is in order-of-magnitude agreement with our estimate.

It therefore follows that the method of periodic pulsed loading and the model for the analysis of the experimental data described above can be used to determine under specific experimental conditions the principal parameters characterizing the microscopic mechanism by means of which a dislocation passes between neighboring valleys of the potential relief: the diffusion coefficient of a kink, its drift velocity, and the effective activation energy for migration along a dislocation line.

We shall now compare the results obtained with the predictions of the theory of Ref. 1. According to Eq. (13), the effective activation energy for the motion of dislocations is  $U_{\text{eff}} = U_k + W_m$ . The values of  $U_{\text{eff}} \approx 2.13$  eV and  $W_m \approx 1.6$  eV deduced from an analysis of the experimental data make it possible to find the energy of a single kink  $U_k \approx 0.53$  eV. This in turn allows us to estimate the Peierls stress  $\sigma_p$ . In the case of a sinusoidal relief, this stress is

$$\sigma_p = \pi^3 U_k^2 / 4a^2 b^2 E_0 \approx 56 \text{ kg/mm}^2, \quad (19)$$

where  $E_0 \approx Gb^2/2$  is the energy per unit length of a dislocation line and  $G$  is the shear modulus.

The Peierls stress divides the regions of thermally activated motion of dislocations in the potential relief from above-barrier motion limited by the viscous-loss mechanism. A comparison of our estimate of  $\sigma_p$  with the experimental values deduced from the measured velocities of dislocations at high stresses shows a large discrepancy between them. Measurements of the velocities of single dislocations in Si single crystals have been carried out so far up to  $\sigma \approx 100$  kg/mm<sup>2</sup>  $> \sigma_p$  (Ref. 16), whereas the characteristics of macroplastic deformation had been investigated in the range of stresses up to  $300$  kg/mm<sup>2</sup>  $\gg \sigma_p$  (Ref. 23). However, none of these experiments has revealed a transition to the range of dislocated motion limited by the mechanism of viscous energy losses.

Apart from serious discrepancies in the estimate of the Peierls stress, there is also disagreement between the theoretically calculated<sup>1</sup> and measured velocity of steady-state motion of dislocations under a static load. Using the value  $U_{\text{eff}} \approx 2.13$  eV, we can calculate the velocity of steady-state motion of dislocations from Eq. (13) for specific experimental conditions. At  $T = 600^\circ\text{C}$  and for  $\sigma = 0.7$  kg/mm<sup>2</sup>, estimates give  $v_d \approx 6 \times 10^{-9}$  cm s<sup>-1</sup>. As pointed out already, the experimentally determined value of the velocity is  $\sim 4 \times 10^{-7}$  cm s<sup>-1</sup>, i.e., there is a considerable (up to two orders of magnitude) discrepancy between the theoretical estimate and the experimentally determined dislocation velocity. It should be pointed out that a similar discrepancy has been reported also in previous papers.<sup>16,3,7</sup> However, it has not yet been possible to determine which of the two fac-

tors [the kink velocity  $v_k$  or the probability of formation of double kink  $J$  given by Eq. (13)] is responsible for the discrepancy. In the present study we were able to determine independently  $J$  and  $v_k$ . A comparison of  $J = 3.5 \times 10^3 \text{ cm}^{-1} \text{ s}^{-1}$ , calculated on the basis of Eq. (10), with  $J = 1.2 \times 10^6 \text{ cm}^{-1} \text{ s}^{-1}$ , estimated from an analysis of the experimental data obtained under conditions of periodic pulsed loading, shows that the concentration of kink pairs on a dislocation line is over two orders of magnitude higher than that calculated on the basis of the theory of Ref. 1.

An additional discrepancy from the theoretical predictions is revealed by an analysis of a possible change in the velocity of dislocations under pulsed loading when the load pulse duration is reduced and the duration of the pauses between the pulses is increased. The minimum value of the dislocation velocity is governed by the concentration  $c_k$  of equilibrium thermal kinks [Eq. (1)] which are present on a dislocation line in the absence of a load. The application of a load causes kinks to drift at a velocity  $v_k$  [Eq. (2)], which sets dislocations in motion at a velocity  $v_d^m$  [Eq. (4)] immediately after the application of the load. The steady-state velocity of dislocation motion during prolong application of a load is given by Eq. (13). The ratio of these velocities

$$v_d^m/v_d \approx \exp \left[ \left( \frac{U_{dk}(\sigma)}{2} - U_k \right) / kT \right] \approx \exp[-(\alpha ab\sigma)^{1/2}/kT] \quad (20)$$

determines the maximum difference between the dislocation velocities when  $t_i$  and  $t_p$  are varied. Substituting the value of  $\alpha$  for  $60^\circ$  dislocations in silicon ( $\alpha = 4.67 \times 10^{-20} \text{ dyn}\cdot\text{cm}^2$ ), we obtain  $v_d^m/v_d \approx 0.58$  for the specific experimental conditions, i.e., the formation and expansion of kink pairs during a load pulse and their relaxation during a pause should alter the dislocation velocity (according to the theory of Ref. 1) in the investigated experimental situation by no more than 40%. This is in conflict with the experimental results presented in Figs. 3 and 4, according to which the measured change in the average glide distance of dislocations during the fixed time of active loading (which corresponds to the average dislocation velocity) is at least two orders of magnitude. It should be pointed out that this conflict cannot be removed by introducing entropy terms,<sup>3,7</sup> which simply alter the equilibrium concentration of kinks and do not affect the ratio  $v_d^m/v_d$ .

The results presented in Figs. 3 and 4 thus can be seen to demonstrate directly that the concentration of kinks on a dislocation differs considerably from the equilibrium value even though the stress may be low, which cannot be explained by the models used in Refs. 1–7 dealing with a homogeneous potential relief and assuming that thermal fluctuations are the main cause of formation of kink pairs.

A higher concentration of kinks on a dislocation line may be due to inhomogeneities of the potential relief created by point defects. It was shown in Refs. 24–26 that point defects increase the probability of formation of double kinks because of a reduction of the barrier hindering their formation by an amount  $U_{dp}$ , which is the energy of the interaction of a dislocation with a point defect. Point defects themselves create barriers  $W_m$  hindering the motion of a kink along a dislocation line. The expression for the effective activation energy of dislocation motion obtained in Refs. 24–26 differs from Eq. (13):  $U_{\text{eff}} \approx 2U_k - U_{dp} + W_m$ . According to these

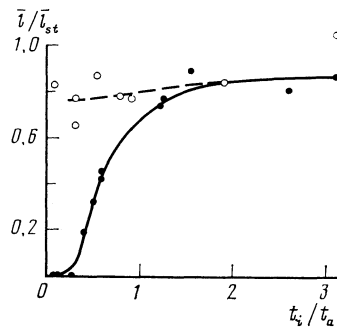


FIG. 9. Normalized average glide distances of dislocations (type 2 in Fig. 2) plotted as a function of the duration of the load pulses (in the case when  $t_p = t_i$ ) for two values of the duration of the leading edge of the pulses: (●)  $t_f = 4 \text{ ms}$ ; (○)  $t_f = 1 \text{ ms}$ ;  $T = 600^\circ\text{C}$ ,  $\sigma = 0.7 \text{ kg/mm}^2$ ,  $\Sigma t_i = t_{st} = 3600 \text{ s}$ .

ideas, the newly formed double kinks are localized at inhomogeneities of the potential relief and contribute to the velocity of dislocations only when a certain minimum stress ensuring the detachment of kinks from pinning centers is applied.

In addition to inhomogeneities of the potential relief, a further source of kink pairs on a dislocation line may be nonlinear excitations of the dynamic soliton type (Fig. 1b). Dynamic solitons (breathers, bions) have been predicted recently on the basis of exact solutions of various nonlinear equations, particularly those describing the behavior of one-dimensional atomic chains.<sup>27</sup> Dynamic solitons by themselves cannot set a dislocation in motion. However, decay of such solitons in the field of external forces may result, because of the dissipative processes, in the appearance of double kinks on a dislocation line and the expansion of these kinks will ensure an increase in the dislocation velocity. It should be pointed out that, according to theoretical estimates, dynamic solitons may appear in an atomic chain only for certain critical amplitudes and rates of application of a load.<sup>28</sup> The processes under discussion have been confirmed by direct experiments involving the observation of dynamic solitons in the magnetic system of a crystal when the applied magnetic field is limited to certain amplitudes and frequencies.<sup>29</sup>

In the case of motion of dislocations under periodic pulsed loading the processes of formation of nonlinear excitations on a dislocation line may be manifested as the leading edge of a load pulse becomes steeper. In our experiments we

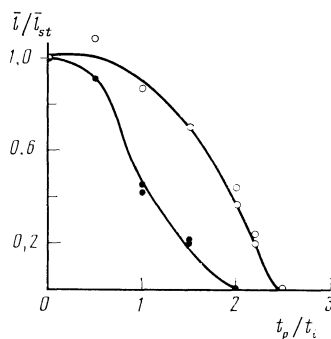


FIG. 10. Dependences of the average glide distances of dislocations (type 2 in Fig. 2) on the duration of pauses in the case when  $t_i/t_a = 0.53$ , obtained for two durations of the leading edge of a load pulse: (●)  $t_f = 4 \text{ ms}$ ; (○)  $t_f = 1 \text{ ms}$ ;  $T = 600^\circ\text{C}$ ,  $\sigma = 0.7 \text{ kg/mm}^2$ .

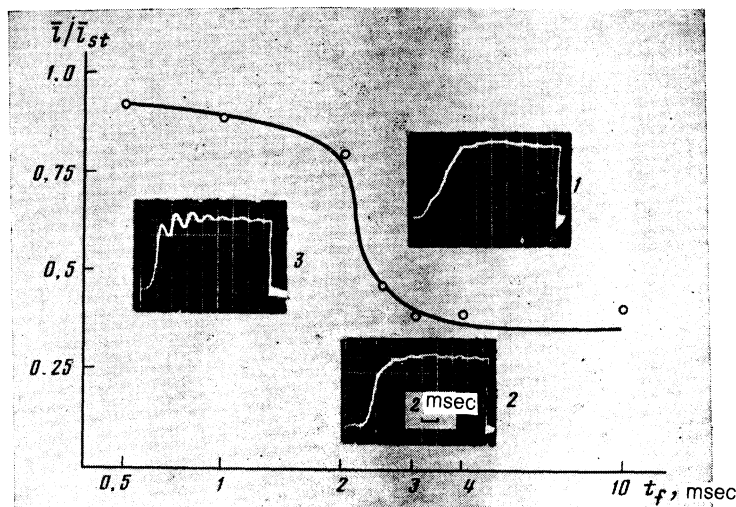


FIG. 11. Average glide distance of dislocations (type 4 in Fig. 2) plotted as a function of the duration of the leading edge of the load pulses ( $t_p = t_i = 30$  ms). The insets show examples of load pulses for  $t_i = 15$  ms: 1)  $t_f = 4$  ms; 2)  $t_f = 2$  ms; 3)  $t_f = 1$  ms;  $T = 600^\circ\text{C}$ ,  $\sigma = 0.7$  kg/mm<sup>2</sup>,  $\Sigma t_i = t_{st} = 3600$  s.

were able to detect the influence of the slope of the leading edge of a pulse on the laws governing the motion of dislocations in the presence of periodic pulsed loading.

Figure 9 shows how the normalized average glide distance of  $60^\circ$  dislocations (of type 2 in Fig. 2) depends on the relative duration of a pulse (at  $t_p = t_i$ ) for two values of the rise time  $t_f$ . Curve 1 corresponds to  $t_f = 4$  ms and curve 2 corresponds to  $t_f = 1$  ms. It is clear that an increase in the slope of the leading edge of a pulse alters the dependence  $\bar{l}(t_i)$ . In the case of relatively smooth loading ( $t_f = 4$  ms) we can expect a monotonic reduction in the distance traveled by dislocations from its static value to zero. When the load is reduced abruptly ( $t_f = 1$  ms), the average glide distance of dislocations decreases slightly (by just 20% relative to the static value) and in the range of short pulse lengths the average glide distance of dislocations is practically independent of  $t_i$ .

Figure 10 shows the dependence of the average glide distance of dislocations of the same  $60^\circ$  type on the length of the pause in the case when  $t_i/t_a = \text{const} = 0.53$  (which corresponds to the position of the point of inflection of curve 1 in Fig. 9). Curve 1 in Fig. 10 was obtained for  $t_f = 4$  ms, whereas curve 2 corresponds to  $t_f = 1$  ms. Clearly, the dependences are qualitatively similar but a decrease in the rise time of the load pulses shifts curve 2 to the right. The point of inflection is located at approximately twice the duration of the pause, compared with curve 1.

Figure 11 shows the dependence of the average glide distance of  $60^\circ$  dislocations (of type 4 in Fig. 2) on the rise time of a pulse for  $t_i = 30$  ms ( $t_i/t_a \approx 0.57$ ) and  $t_p = t_i$ . We can see that in the interval from 10 to 3 ms the average glide distance of dislocations is practically independent of  $t_f$  and as the rise time of the load pulses further decreases this distance rises nonlinearly with reduction in the pulse length. Similar dependences  $\bar{l}(t_f)$  are observed for other types of dislocations. The insets show typical load pulses in the case when the leading edge is 4 ms (1), 2 ms (2), and 1 ms (3). It is clear from the oscillograms in Fig. 11 that an increase in the slope of the leading edge of the load pulses alters somewhat the pulse profile. In the initial part of the peak of a pulse with  $t_f = 1$  ms we observed oscillations at the natural frequency of the components of the loading system and of the

sample. A major change in the average glide distance traveled by a dislocation was however observed at  $t_f \approx 2-3$  ms, when the pulse profile changed only slightly and it differed little from the case when  $t_f = 4$  ms. Moreover, special experiments in which such oscillations were excited relative to the static load confirmed that a brief excess of the load above the average value did not alter significantly the velocity of the steady-state motion of dislocations.

The results presented in Figs. 9-11 thus demonstrate convincingly that a decrease in the rise time of the load pulses activates an additional source of kink pairs ensuring a macroscopic displacement of a dislocation even in those cases when its velocity, limited by the processes of thermal-fluctuation formation of double kinks, is zero. This additional channel of appearance of stable kink pairs in the system is due to the combined influence of inhomogeneities of the Peierls relief and the processes of excitation in a system of nonlinear waves (dynamic solitons) and their relaxation. Clearly, these assumptions should make it possible to eliminate the discrepancies between the theoretical predictions and experimental data. However, it must be pointed out that a theoretical analysis of the processes of formation and characteristics of such solitary waves in a three-dimensional system of vibrating atoms is not yet available.

The authors are grateful to V. M. Vinokur, V. L. Indenbom, V. Ya. Kravchenko, B. V. Petukhov, and V. L. Pokrovskii for their interest and valuable discussions.

<sup>1</sup>J. P. Hirth and J. Lothe, *Theory of Dislocations*, Wiley, New York (1968).

<sup>2</sup>A. P. Kazantsev and V. L. Pokrovskii, *Zh. Eksp. Teor. Fiz.* **58**, 677 (1970) [*Sov. Phys. JETP* **31**, 362 (1970)].

<sup>3</sup>Y. Kawata and S. Ishioka, *Philos. Mag.* **A 48**, 921 (1983).

<sup>4</sup>B. V. Petukhov and V. L. Pokrovskii, *Zh. Eksp. Teor. Fiz.* **63**, 634 (1972) [*Sov. Phys. JETP* **36**, 336 (1973)].

<sup>5</sup>A. Seeger, *J. Phys. (Paris)* **42**, Colloq. 5, C5-201 (1981).

<sup>6</sup>M. Büttiker and R. Landauer, *Phys. Rev.* **A 23**, 1397 (1981).

<sup>7</sup>M. Heggie and R. Jones, *Philos. Mag.* **A 48**, 365 (1983).

<sup>8</sup>M. N. Kabler, *Phys. Rev.* **131**, 54 (1963).

<sup>9</sup>V. N. Erofeev, V. I. Nikitenko, and V. B. Osvenskii, *Phys. Status Solidi* **35**, 79 (1969).

<sup>10</sup>A. George, C. Escaravage, G. Champier, and W. Schröter, *Phys. Status Solidi B* **53**, 483 (1972).

<sup>11</sup>J. R. Patel, L. R. Testardi, and P. E. Freeland, *Phys. Rev. B* **13**, 3548 (1976).

- <sup>12</sup>B. Ya. Farber and V. I. Nikitenko, *Phys. Status Solidi A* **73**, K141 (1982).
- <sup>13</sup>M. Imai and K. Sumino, *Philos. Mag. A* **47**, 599 (1983).
- <sup>14</sup>H. Schaumburg, *Philos. Mag.* **25**, 1429 (1972).
- <sup>15</sup>I. E. Bondarenko, V. N. Erofeev, and V. I. Nikitenko, *Zh. Eksp. Teor. Fiz.* **64**, 2196 (1973) [*Sov. Phys. JETP* **37**, 1109 (1973)].
- <sup>16</sup>V. N. Erofeev and V. I. Nikitenko, *Zh. Eksp. Teor. Fiz.* **60**, 1780 (1971) [*Sov. Phys. JETP* **33**, 963 (1971)].
- <sup>17</sup>V. I. Nikitenko, *Dynamics of Dislocations* [in Russian], Naukova Dumka, Kiev (1975), p. 7.
- <sup>18</sup>V. I. Nikitenko and B. Ya. Farber, in: *Dislocations in Solids* (Proc. Ninth Yamada Conf., Tokyo, 1984, ed. by H. Suzuki, T. Nimomiya, K. Sumino, and S. Takeuchi), University of Tokyo Press (1985), p. 417.
- <sup>19</sup>V. I. Nikitenko, B. Ya. Farber, and Yu. L. Iunin, *Pis'ma Zh. Eksp. Teor. Fiz.* **41**, 103 (1985) [*JETP Lett.* **41**, 124 (1985)].
- <sup>20</sup>B. Ya. Farber, Yu. L. Iunin, and V. I. Nikitenko, *Phys. Status Solidi A* **97**, 469 (1986).
- <sup>21</sup>V. N. Erofeev, V. I. Nikitenko, V. I. Polovinkina, and É. V. Suvorov, *Kristallografiya* **16**, 190 (1971) [*Sov. Phys. Crystallogr.* **16**, 151 (1971)].
- <sup>22</sup>V. I. Nikitenko, B. Ya. Farber, and E. V. Yakimov, *Cryst. Res. Technol.* **19**, 295 (1984).
- <sup>23</sup>J. Rabier, P. Veyssiere, and J. L. Demenet, *J. Phys. (Paris)* **44**, Colloq. 4, C4-243 (1983).
- <sup>24</sup>V. Celli, M. Kabler, T. Ninomiya, and R. Thomson, *Phys. Rev.* **131**, 58 (1963).
- <sup>25</sup>B. V. Petukhov, *Fiz. Tverd. Tela (Leningrad)* **24**, 439 (1982) [*Sov. Phys. Solid State* **24**, 248 (1982)].
- <sup>26</sup>B. V. Petukhov, *Fiz. Tverd. Tela (Leningrad)* **25**, 1822 (1983) [*Sov. Phys. Solid State* **25**, 1048 (1983)].
- <sup>27</sup>M. Toda, *Theory of Nonlinear Lattices*, Springer Verlag, Berlin (1981) [Springer Series in Solid-State Sciences, Vol. 20].
- <sup>28</sup>J. H. Batteah and J. D. Powell, in: *Solitons in Action* (Proc. Workshop, Redstone Arsenal, 1977, ed. by K. Lonngren and A. Scott), Academic Press, New York (1978), p. 257.
- <sup>29</sup>V. I. Nikitenko, L. M. Dedukh, and V. K. Vlasko-Vlasov, in: *Dislocations in Solids* (Proc. Ninth Yamada Conf., Tokyo, 1984, ed. by H. Suzuki, T. Nimomiya, K. Sunino, and S. Takeuchi), University of Tokyo Press (1985), p. 493.

Translated by A. Tybulewicz